

Chapter 4

Iris Recognition in the Framework of Quantum-behaved Particle Swarm Optimization

In chapter 3, a fast and efficient iris segmentation approach has been presented. The computation of algorithmic parameters such as threshold values for image binarization is usually based on fixed values. It is database dependent and is not found to be suitable for all kinds of iris images. This chapter presents an optimal threshold value selection method based on Quantum-behaved Particle Swarm Optimization (QPSO) for proper segmentation of an iris from a given eye image. The chapter also presents a hybrid iris recognition algorithm based on Artificial Neural Network (ANN) and city block distance. The iris recognition system performance both in iris identification and verification mode are analyzed and presented in this chapter.

4.1 Introduction

Biometric is a science of recognizing a person based on physiological and behavioral characteristic (Nabti *et al.*, 2008). Among the various biometric techniques *viz.* face, iris, fingerprint, palm print, Gait, recognition based on iris image is the most reliable and promising for high-security environment due to the unique, stable, non-invasive characteristics of the iris. In iris recognition system, segmentation is the vital and time-consuming step for the overall performance of the system. Iris part should be properly segmented and be free from artifacts such as eyelids, eyelashes, reflections etc. so that extracted iris features have high discriminating capability.

Due to the simplicity of thresholding method, it is commonly used in the iris segmentation in order to detect pupil, iris, eyelashes and reflections. It is a suitable technique for detection of specular reflections, multiple eyelashes over non-ideal eye images as compared with the state of art methods based on edge detection approach which may not suit these purposes. But, the efficacy of the thresholding method is based on the threshold value. The selection of optimal threshold value is the fundamental steps for thresholding (Patra *et al.*, 2014). Various authors have adopted the thresholding method during iris segmentation. The authors either used ‘trial and error’ or ‘statistical decision making’ approach for the selection of optimal threshold value. Al-Zubi *et al.* (2007), Kalka *et al.* (2010) applied thresholding with value ‘100’ and ‘240’ on the eye images to isolate eyelashes and reflections, respectively. De Marsiko *et al.*, (2011) applied ‘150’ as a threshold value to isolate the pupil region. Raffei *et al.*, (2013) used value ‘20’ as a threshold value to isolate eyelashes. Ziauddin *et al.* (2009) adopted thresholding to segment pupil region. Here, the threshold value T is determined as $T = i + \max(20, 0.4 * i)$, where, i is the selected intensity value such that the number of points with intensity below i is greater than 0.1% of the total image area. Shah *et al.* (2009) isolate pupil region by thresholding with minimum pixel value plus a constant value ‘25’ as threshold value. Ghodrati *et al.*, (2014) applied statistical decision making algorithm for finding the appropriate threshold value for eyelashes and reflection detection. Ferone *et al.* (2014) adopted Otsu thresholding procedure to obtain the threshold values. These existing thresholding methods are database dependent and may not be suitable for all kinds of iris images.

In order to develop a database independent thresholding method and to overcome the difficulty of the selection of optimal threshold value for iris segmentation, a Quantum Behaved Particle Swarm Optimization (QPSO) based approach has been proposed in this chapter. A hybrid iris image recognition approach based on ANN and city block distance has also been presented in this chapter. The proposed QPSO based iris recognition approach with experimental results is presented in the following sections.

4.2 Proposed Iris Recognition Approach

The proposed iris image recognition approach consists of two phase *viz.* Enrolment phase and Recognition phase. During enrolment phase, features are extracted from segmented iris and store in the database as a reference. For proper segmentation of an iris from a given eye image, QPSO based threshold value selection method has been used. During recognition phase, extracted features from query iris image are compared with stored features to recognize the query iris. A hybrid iris recognition algorithm based on Artificial Neural Network (ANN) and city block distance has been used for iris recognition. The proposed iris recognition approach in the framework of QPSO is shown in Figure 4.1.

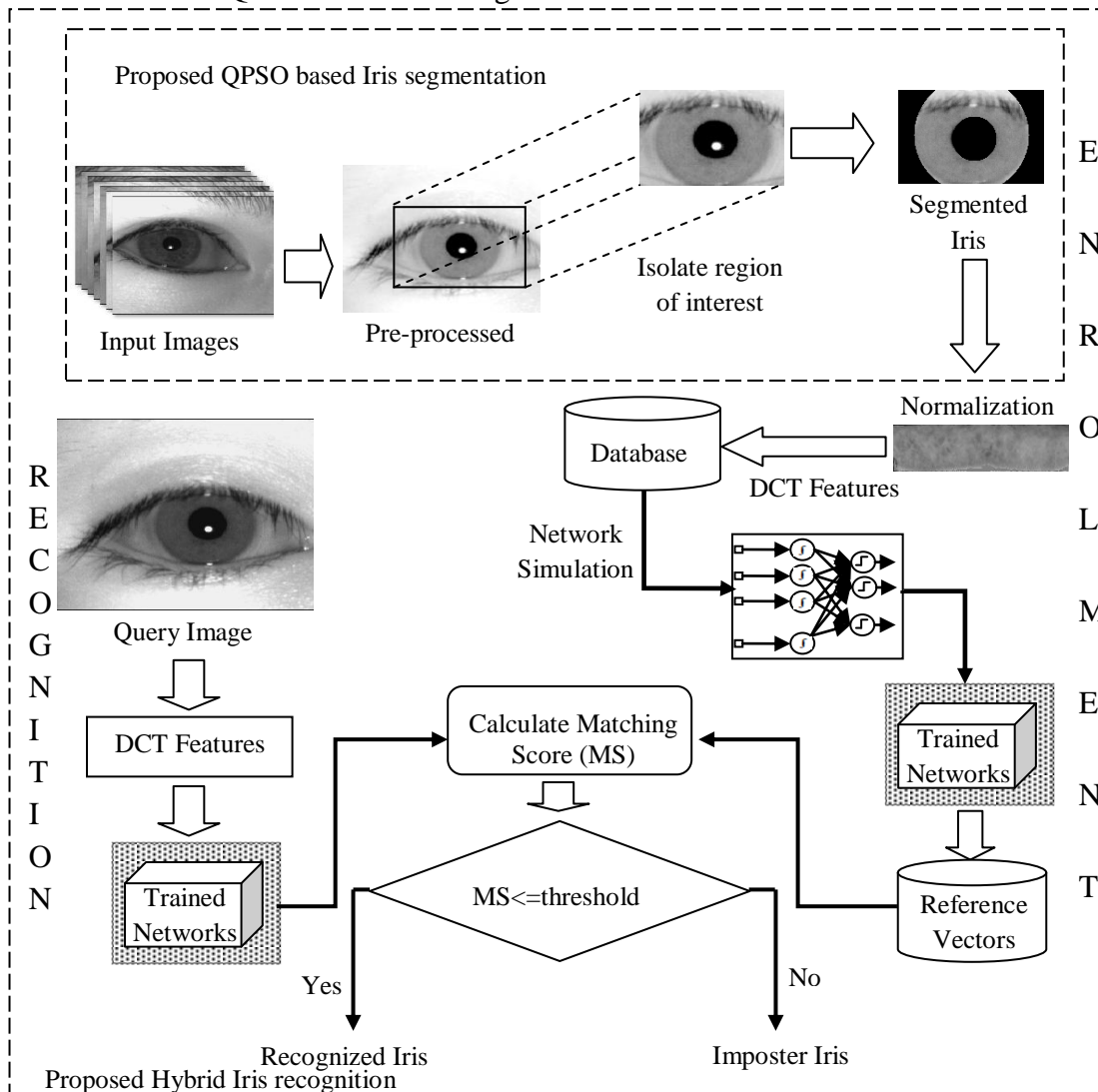


Figure 4.1 Proposed iris recognition approach

The proposed approach consisting of the following steps is depicted in Figure 4.2:
 (i) Pre-Processing (ii) Determination of threshold values (iii) Isolation of expected eye region
 (iv) QPSO based Segmentation (v) Normalization (vi) Noise Reduction (vii)
 Extraction of Iris Features and (viii) Iris Recognition based on hybrid algorithm.

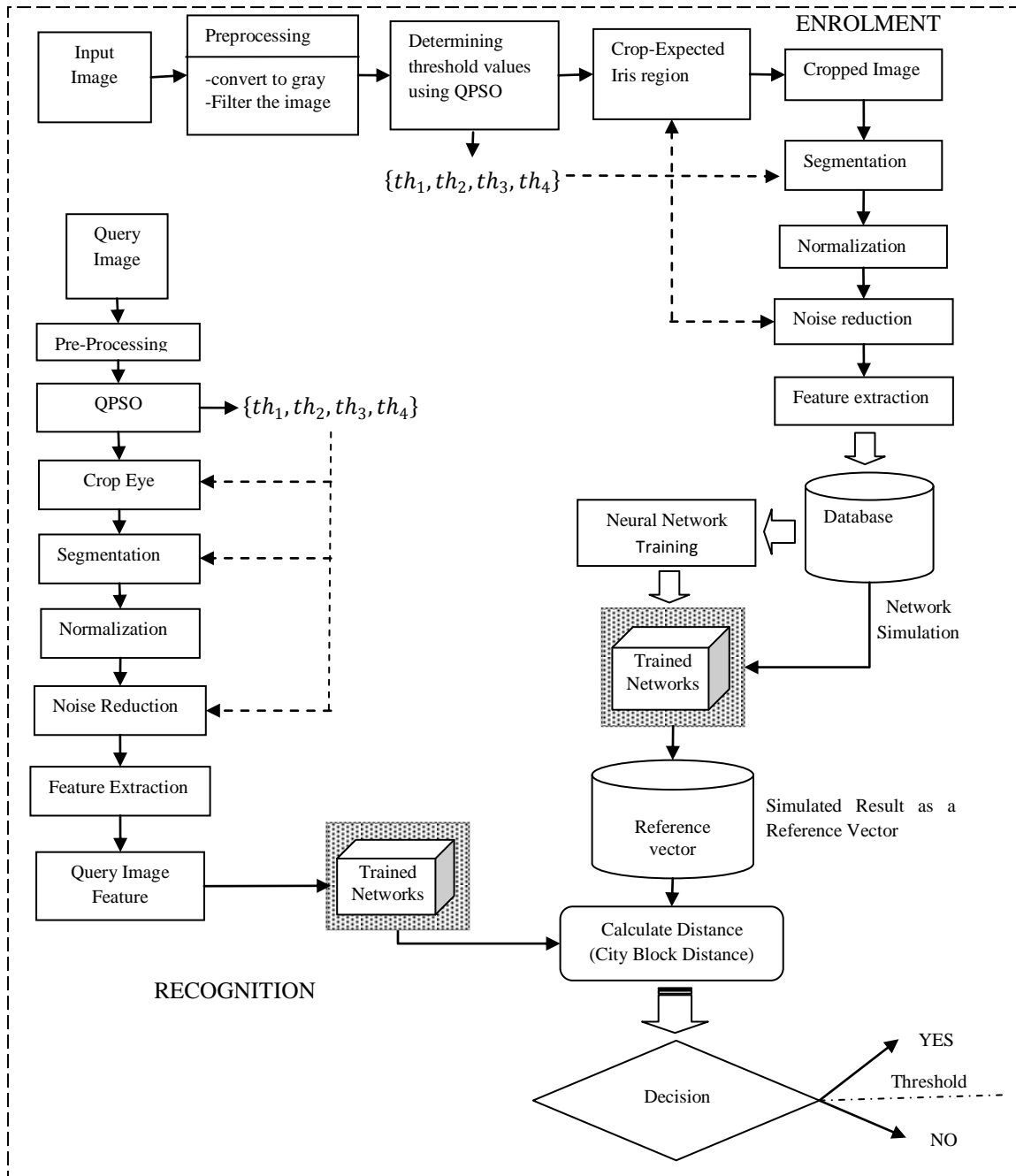


Figure 4.2 Steps of the proposed iris recognition approach

On acquiring iris image for recognition, pre-processing is done to enhance the image quality. The linear thresholding method is usually used in different iris recognition algorithms in order to detect pupil region, iris region or to remove reflections, eyelashes, eyelids etc. But the efficiency of the thresholding method is found to be dependent on the threshold value. To overcome this difficulty, it is proposed to apply QPSO to select an optimal threshold value for linear thresholding on the input image. Therefore, before performing segmentation, the threshold values for the input image are obtained using QPSO. With these threshold values, probable eye region of interest is isolated from rest of the images by linear thresholding. The segmented iris image is then normalized and the artifacts are removed from it. The unique features are extracted from each of the normalized images and stored in the database. During enrolment, neural network system composes of 7 feed-forward neural networks are trained and simulated with these stored features. The network output vectors are stored as reference vector. During recognition, query features are fed into trained network system to obtain network output vector. Next, matching score (MS), City block distance, is calculated between output vector and the reference vector. The person is identified based on the value of MS less than or equal to a threshold value. Threshold value equal to 0.11 is obtained through the experiments based on False Acceptance Rate (FAR) and False Rejection Rate (FRR) of the system. For verification, MS is calculated between network vector and target vector. Each of the steps in the proposed approach is described in detail in the following sections.

4.2.1 Pre-processing

The iris image acquired for recognition may have a shadow or low contrast, as shown in Figure 4.3 (a), which may affect the segmentation and feature extraction process. Therefore, enhancement is necessary prior to further processing of the acquired iris images. Multi-Scale Retinex (MSR) filter is adopted which enhances the local contrast of a given image without sacrificing color rendition and dynamic range compression (Petro *et al.*, 2014).

The MSR is defined by equation (4.1) (Proenca *et al.*, 2010):

$$F_i(x, y) = \sum_{n=1}^N W_n * \{\log[S_i(x, y) * M_n(x, y)]\} \quad (4.1)$$

where, $F_i(x, y)$ is a filtered image, $S_i(x, y)$ is an input image, $i \in R, G, B$ represents three colour bands, N stands for number of scales being used, W_n are the weighting factors for the n scales. $M_n(x, y)$ is the surround function given by equation (4.2):

$$M_n(x, y) = K_n e^{-(x^2+y^2)/\sigma_n^2} \quad (4.2)$$

where, the σ represents the standard deviation of the Gaussian distribution that determine the scale. K_n is a normalization factor given by equation (4.3):

$$K_n = \frac{1}{\sum_{x,y} F_n(x, y)} \quad (4.3)$$

The result of MSR filtering on different images is shown in Figure 4.3 (b).

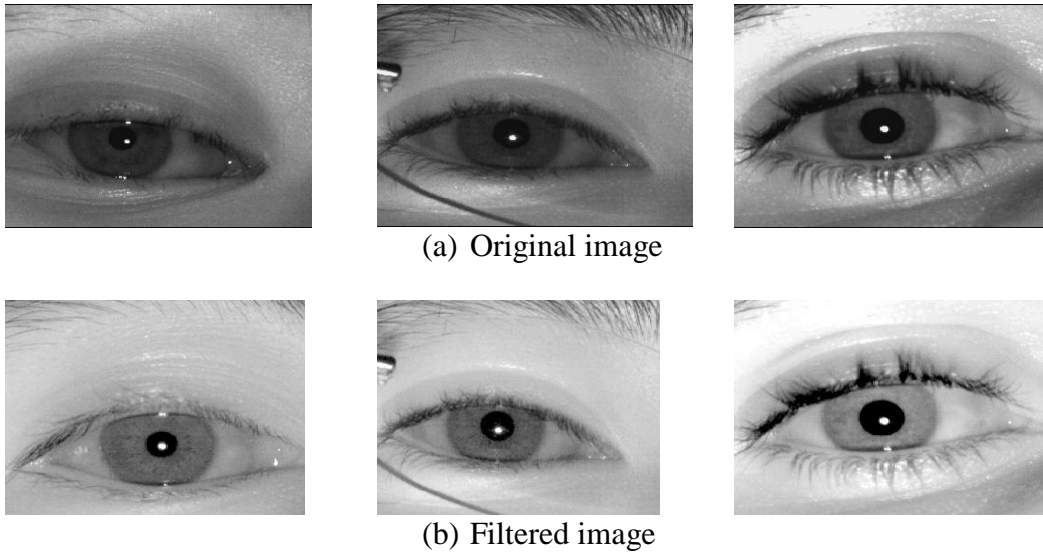


Figure 4.3 Results of the MSR filtering

4.2.2 Determination of Threshold Values

The optimal threshold values from filtered image are obtained by using QPSO which is a quantum model of Particle Swarm Optimization (PSO). Unlike in PSO in

which state of a particle is depicted by position and velocity, the state of a particle in QPSO is depicted by the wave function (Omkar *et al.*, 2009). In QPSO, if the position of i^{th} particle at t^{th} iteration is expressed as $X_i(t)$, $i = 1, 2, \dots, N$, the particle's position is updated according to the equation (4.4) and equation (4.5):

$$X_i(t + 1) = P_i - \beta * (mBest - X_i(t)) * \ln(1/u) \text{ if } k \geq 0.5 \quad (4.4)$$

$$X_i(t + 1) = P_i + \beta * (mBest - X_i(t)) * \ln(1/u) \text{ if } k < 0.5 \quad (4.5)$$

where,

$$P_i = \varphi * pBest_i + (1 - \varphi) * gBest_i \quad (4.6)$$

$$mBest = \frac{1}{N} \sum_{i=1}^N pBest_i \quad (4.7)$$

N represents a total number of particle, $mBest$ is the mean of all the best position of the population, u, k and φ are the random numbers distributed uniformly over $[0, 1]$ respectively. The β is called as Contraction-Expansion coefficient, only parameter in the QPSO which can be tuned to control the convergence speed of the algorithm. $gBest_i$ is the global best position of i^{th} particle until $(t - 1)^{th}$ iteration. $pBest_i$ is the previous best position of i^{th} particle until $(t - 1)^{th}$ iteration. P_i is the global extremum of the i^{th} particle.

The particles in the QPSO are evaluated with the fitness function based on the between-class variance σ_B^2 of the image intensity distribution which is a measure of separability between classes and it gives the optimal global threshold value. The function is defined by equation (4.8):

$$fitness_V = \max(\sigma_B^2(th_j)) \quad (4.8)$$

where, th_j stands for threshold levels, $j = 1, 2, \dots, 5$.

The σ_B^2 is defined by equation (4.9):

$$\sigma_B^2 = \sum_{j=1}^5 w_j (\mu_j - \mu_t)^2 \quad (4.9)$$

Here, j represents a specific class, w_j and μ_j are the probability of occurrence and mean of class j , respectively. The probability of occurrence is given by equation (4.10):

$$w_j = \begin{cases} \sum_{i=1}^{th_j} p_i, & j = 1 \\ \sum_{i=th_{j-1}+1}^{th_j} p_i & 1 < j < n \\ \sum_{i=th_{j-1}+1}^L p_i & j = n \end{cases} \quad (4.10)$$

The mean of each class is given by equation (4.11):

$$\mu_j = \begin{cases} \sum_{i=1}^{th_j} \frac{ip_i}{w_j}, & j = 1 \\ \sum_{i=th_{j-1}+1}^{th_j} \frac{ip_i}{w_j} & 1 < j < n \\ \sum_{i=th_{j-1}+1}^L \frac{ip_i}{w_j} & j = n \end{cases} \quad (4.11)$$

μ_t represents total mean of the image and calculated by equation (4.12):

$$\mu_t = \sum_{i=1}^L ip_i \quad (4.12)$$

where, L is intensity levels in the given gray image in the range $\{0, 1, 2, \dots, 255\}$, i represents a specific intensity level, i.e., $0 \leq i \leq 255$. p_i stands for probability distribution i^{th} intensity level and is calculated by equation (4.13):

$$p_i = \frac{h_i}{M} \quad (4.13)$$

where, M represents the total number of pixels in the image, h_i is the image histogram.

The Algorithm 4.1 describes the QPSO based selection of optimal threshold values.

Algorithm 4.1: Selection of optimal threshold values using QPSO

Input: Histogram of the gray eye image

Output: Optimal threshold values, $[th_1, th_2, th_3, th_4]$.

Termination criteria: Number of generation or error factor

The steps involved in the selection of optimal threshold value using QPSO are:

- i) Generate initial position of particles.
 - ii) Compute the fitness value of each particle using equation (4.8) and store
-

Algorithm 4.1: Selection of optimal threshold values using QPSO (Continued...)

- the best fitness value along with its string Sp .
- iii) Update the position of particles using equation (4.4) and (4.5).
 - iv) Determine best fitness value by comparing the best string of current particle Sc with best string in previous particle Ps .
 - v) If the fitness value of string $Sc < Sp$, then replace Sp with Sc . Repeat step ii) to iv) until termination criteria is reached.
-

The optimal threshold values i.e. $[th_1, th_2, th_3, th_4]$ returned by Algorithm 4.1 are used for accurate segmentation of iris region from rest of an eye image. The threshold value th_1 represents pupil and eyelashes, th_2 represents iris region, th_3 and th_4 represents sclera and skin region and pixel value greater than th_4 represents reflections respectively.

4.2.3 Isolation of Expected Eye Region

In this step, expected region of an eye is isolated from rest of the image. This reduces the size of the image which in turn reduces the processing time of the system. First, input image is converted to binary image by linear thresholding with threshold value th_1 . The centroid of the binary object is determined after performing morphological operations on the binary image. A rectangular region around the centroid is isolated from the rest of the image which is expected to be eye region of interest as shown in Figure 4.4.

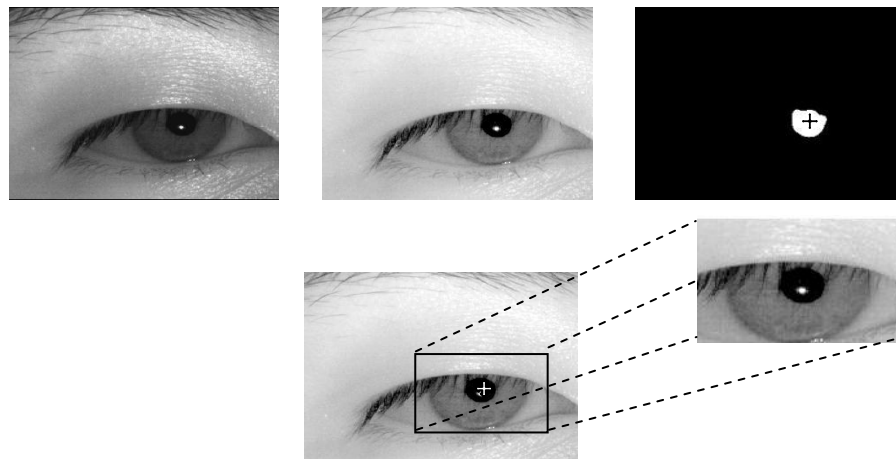


Figure 4.4 Isolation of the expected eye region

4.2.4 QPSO based Segmentation

The segmentation of iris is performed on the isolated eye region. This step consists of detection of inner and outer iris boundaries, reduction of noise such as reflection, eyelids and eyelashes. As iris size varies from one image to other, normalization is needed to obtain the uniform size of the iris image. Normalization is performed before the noise reduction step. The segmentation process is described next.

4.2.4.1 Detection of Outer Boundary

The detection of an iris outer boundary, i.e. sclera boundary, on a given input image is performed in two phases:

- (a) Approximation of radius and centre co-ordinates
- (b) Determination of actual radius and centre co-ordinates

In phase (a), the approximated radius and centre co-ordinates of an iris outer boundary is calculated by using circle geometry. The actual radius and centre co-ordinates are obtained by using Circular Hough Transformation (CHT) in phase (b) with the help of outputs returned by the first phase. The phase (a) and (b) are described next.

(a) Approximation of radius and centre co-ordinates

The approximated radius and centre co-ordinates based on circle geometry are calculated by using Algorithm 4.2.

Algorithm 4.2: Calculation of an approximated radius and centre co-ordinates

Input: Isolated eye image, I

Output: Approximated radius, r_a , and centre co-ordinates, $C_a(x,y)$ of iris outer boundary.

- i. Create binary image of the input image by linear thresholding with threshold value th_1 .
 - ii. Perform morphological operations and median filtering on the resultant image
 - iii. Obtain centroid, $C_{x,y}$ of the binary object. Two subparts of the iris image is selected as follows:
 - a) From $C_{x,y}$, move towards left and count number of 1's (say c_l), stop when first is zero encounter.
 - b) Similarly, move towards right from $C_{x,y}$ and count number of 1's
-

**Algorithm 4.2: Calculation of an approximated radius and centre co-ordinates
(Continued...)**

(say c_r), stop when first is zero encounter.

c) Two sub-parts img_1 and img_2 selected as:

$$img_1 = I(C_{x,y}(2):end, 1:(C_{x,y}(1) - c_l) - 1) \text{ and}$$

$$img_2 = I(C_{x,y}(2):end, 1:(C_{x,y}(1) + c_r) + 1) \text{ as shown in Figure 4.5(c)}$$

iv. Obtain three vertical points in the img_1 and img_2 by using canny edge detection method and linear Hough Transform. Fit the curve through these detected points by using circle geometry. The circle geometry returns approximated centre co-ordinates $C_a(x,y)$ and radius r_a of the iris outer boundary as shown in Figure 4.5(d).

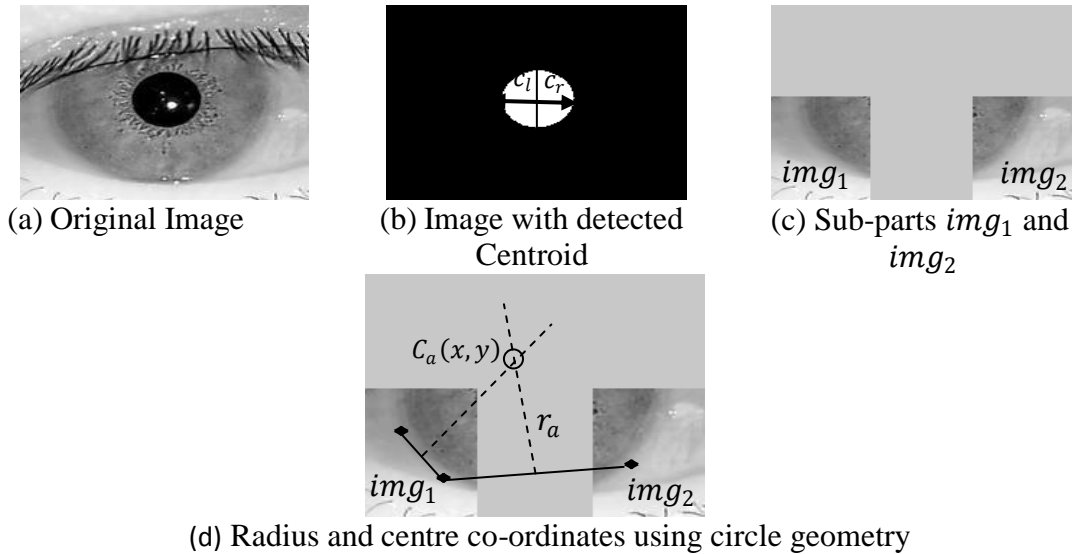


Figure 4.5 Calculation of an approximated radius and centre co-ordinates using circle geometry

(b) Determination of actual radius and centre co-ordinates

The actual iris radius, r_i and centre co-ordinates $C_i(a,b)$ are obtained by using canny edge detection method and CHT (Masek *et al.*, 2003). The CHT search a circle on the image with radius margin of $r_a \pm 5$. This step fixes any dislocation of outer boundary obtained during circle geometry process. The CHT depends on the equation of the circle, equation (4.14):

$$r^2 = (x - a)^2 + (y - b)^2 \quad (4.14)$$

where, a and b represents centre co-ordinates, x and y represent edge point and r represent radius of circle respectively. The parametric definition of circle is (equation 4.15):

$$\begin{aligned} x &= a + r * \cos(\theta) \\ y &= b + r * \sin(\theta) \end{aligned} \tag{4.15}$$

A circle is drawn with each edge point as origin and radius r . The centre co-ordinates and radius are stored in 3-dimensional accumulator array. The value of an accumulator array is increased every time a circle is drawn over every edge point with desired centre co-ordinates and radii. The accumulator keeps the count of how many circle pass through coordinates of each edge point and select the centre coordinates of the circle in the image with the highest count. With precise range of radius and accurate edge points, the CHT will perform well in terms of computational time for detecting circle in the image. Keeping this in consideration, Canny Edge Detection method and hybrid of circle geometry and CHT is used. In this present work, CHT searches centre coordinates of the circle with precise radius range ($r_a \pm 5$) given by circle geometry through the edge points returned by the canny method. With this precise range of radius ($r_a \pm 5$), the computational time of the CHT is significantly improved.

4.2.4.2 Detection of Inner Boundary

The detection of iris inner boundary, i.e. pupillary boundary, is performed on the given input image by using Algorithm 4.3.

Algorithm 4.3: Detection of inner Boundary

Input: Eye image, I , with detected iris outer boundary.

Output: Centre Coordinates $C_p(x, y)$ and radius r_p of pupil.

- i. Isolate a small rectangle around the centroid within iris outer boundary.
 - ii. Apply canny to detect edge points on the image.
 - iii. Apply CHT is to find the circle parameters ($C_p(x, y)$ and r_p).
-

4.2.4.3 Normalization

Due to varying size of iris from one image to other, the normalization is performed to obtain the uniform size. Daugman' Rubber sheet model has been applied

to perform normalization of the segmented iris. Each point within the segmented iris is transformed to the polar coordinates (r, θ) , where r is on the interval $[0, 1]$ and θ is an angle in $[0, 2\pi]$, by using equation (4.16) (Daugman, 2004):

$$\begin{aligned} x &= x_c + r\cos(\theta) \\ y &= y_c + r\sin(\theta) \end{aligned} \quad (4.16)$$

where, (x_c, y_c) denotes coordinates of centre of the iris and (x, y) denotes coordinates of the points on the circle respectively. Most of the time, it is seen that the upper part of the iris is fully or partially covered by top eyelid. So, in this present work, upper iris part is ignored during normalization process as shown in Figure 4.6.

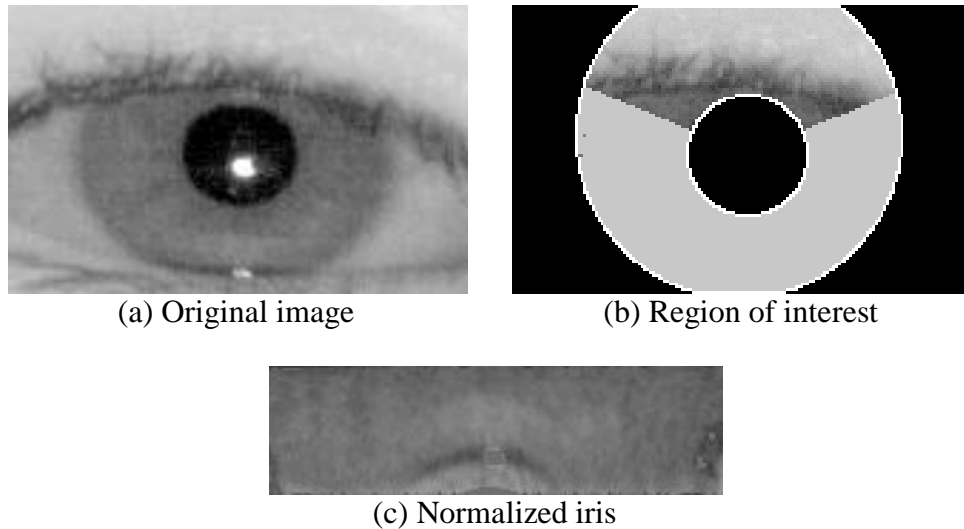
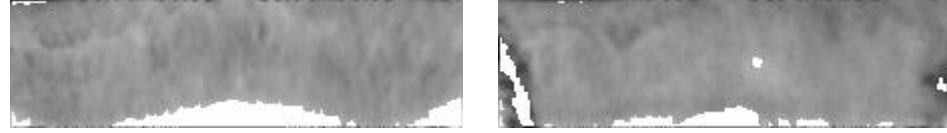


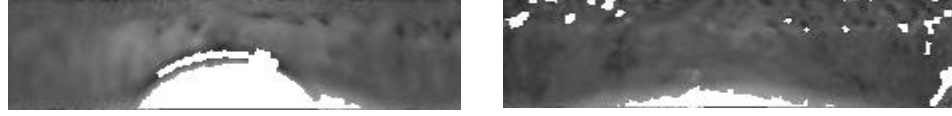
Figure 4.6 Normalization process

4.2.4.4 Noise Reduction

The artifacts such as eyelids, eyelashes and reflections on the normalized iris image are removed by using linear thresholding with the help of optimal threshold values returned by the Algorithm 4.1. The pixel of the iris image less than or equal to the threshold value th_1 is supposed to be eyelashes, pixel value greater than or equal to th_3 represents eyelids and pixel values greater than th_4 represent the reflections over normalized iris image respectively. With appropriate threshold value, these artifacts are removed from the normalized iris image by using linear thresholding. The result of the linear thresholding over the MMU2 (MMU2 Iris Database, 2010) and IIT Delhi (IITD Iris Database, 2008) iris dataset is shown in Figure 4.7.



(a) MMU2 Dataset



(b) IIT Delhi Dataset

Figure 4.7 Normalized iris with the detected noise

4.2.5 Extraction of Iris Features

The unique texture features are extracted from normalized iris image to represent each image with a minimum dimensionality. The DCT technique has been adopted to extract the unique features from the normalized iris images. The DCT is an image processing technique which transforms image from the spatial domain into frequency domain. When DCT is applied on the image, the most of the signal information are compressed into some coefficient. Considering this energy compaction property, DCT is chosen for extraction of a feature from iris templates. When DCT is applied on the iris image $I_{x,y}$ of dimension, $m \times n$, it returns the coefficient matrix, $D_{u,v}$ of low frequency and high frequency of same dimension $m \times n$ (Sarhan *et al.*, 2009). The $D_{u,v}$ is calculated by equation (4.17):

$$D_{u,v} = \frac{1}{\sqrt{mn}} \alpha(u) \alpha(v) \sum_{x=0}^{m-1} \sum_{y=0}^{n-1} I_{x,y} \times \cos\left(\frac{(2x+1)u\pi}{2m}\right) \times \cos\left(\frac{(2y+1)v\pi}{2n}\right) \quad u = 0, 1, \dots, m, v = 0, 1, \dots, n \quad (4.17)$$

where, $\alpha(a)$ is calculated by equation (4.18):

$$\alpha(a) = \begin{cases} \frac{1}{\sqrt{2}} & a = 0 \\ 1 & \text{otherwise} \end{cases} \quad (4.18)$$

The feature vector of each image is generated by selecting low-frequency DCT coefficient from top left corner of the matrix, $D_{u,v}$, using zonal selection method as described by Algorithm 4.4.

Algorithm 4.4: Feature Extraction

Input: Normalized iris image of size $[64 \times 224]$

Output: Extracted iris feature, I_f .

- i. Read iris image and enhanced with Adaptive Histogram Equalization (AHE)
- ii. Subtract 128 from enhanced image.
- iii. Calculate DCT coefficient of the whole resultant image and select the coefficients, α , with a zonal mask of size $[3 \times 3]$.
- iv. Again, a resultant image obtained in step ii is divided into 14 blocks of size $[32 \times 32]$ each.
- v. Calculate DCT coefficient of each block.
- vi. Select the DCT coefficient, β_i , ($i = 1, 2, \dots, 14$), with zonal mask of size $[2 \times 2]$ similar to step iii.
- vii. Combine the α and β_i , ($i = 1, 2, \dots, 14$) to obtain iris features, I_f .

$$I_f = [\alpha \beta_i], \quad (i = 1, 2, \dots, 14)$$

There is 65 number of DCT coefficient in each I_f and the feature vector, f_{vector} , is constructed by combining I_f obtained from each image of the dataset. By varying the size of zonal mask from $[1 \times 1]$ to $[4 \times 4]$, f_{vector} is also constructed and analyzed to assess the suitability of f_{vector} on recognition performance.

4.2.6 Iris Recognition based on Hybrid Algorithm

Different iris recognition approaches *viz.* Al-allaf *et al.* (2012) and Mozumder *et al.* (2015) adopted single all-encompassing Multi-Layer Perceptron neural network, which is susceptible to the size of the database. To overcome this problem, a hybrid ensemble of feed-forward neural network and statistical city block distance is proposed to be used for iris image recognition. The proposed hybrid approach for iris image recognition is shown in Figure 4.8. A module of n ($n = 7$) neural networks is trained with f_{vector} . The f_{vector} is equally divided among the n neural networks during training and then trained network system is simulated with f_{vector} . The network output vectors

are stored as reference vector, f_{ref} . During recognition, query features, q_f , are fed into trained network system to obtain network output vectors, y_q . Next, the MS is calculated between output vector and reference vector.

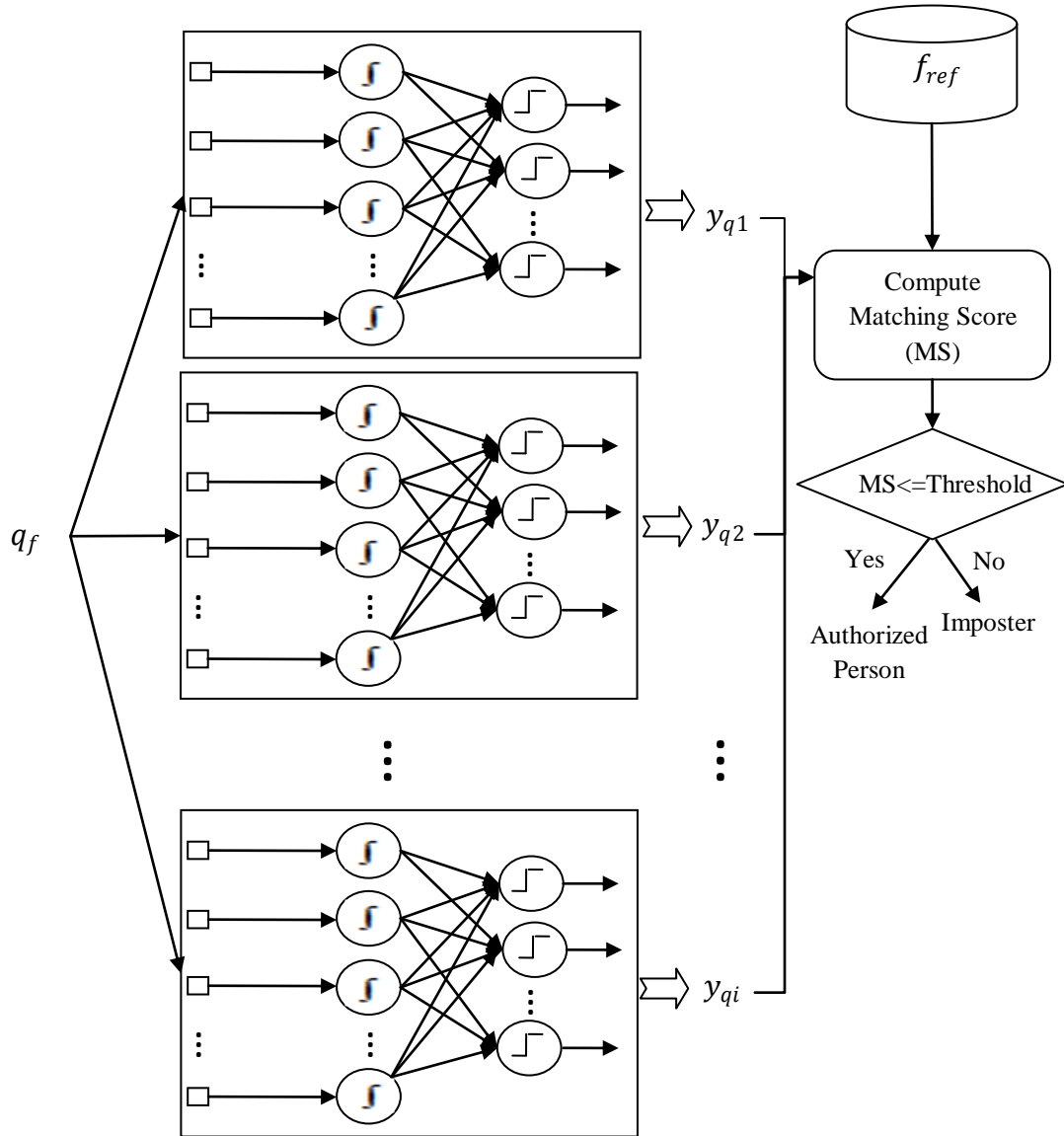


Figure 4.8 Proposed hybrid iris recognition approach

The person is identified based on value of MS less than or equal to threshold value. For verification, MS is calculated between network vector and target vector. The system recognizes the query image, $Q_{i,j}$, by equation (4.19):

$$Q_{i,j} = \begin{cases} \text{Recognized} & \min \left(d \left(y_{qi}, f_{ref}(i,j) \right) \right) \leq \text{threshold} \\ \text{Imposter} & \text{otherwise} \end{cases} \quad (4.19)$$

$i = 1, 2, \dots, 7 \text{ and } j = 1, 2, \dots, 40$

The $Q_{i,j}$ can be read as query image I belonging to i^{th} network of j^{th} image. The $d(y_q, f_{ref})$ represents the MS between y_q and f_{ref} defined by equation (4.20):

$$d(y_{qi}, f_{ref}(i,j)) = |y_{qi} - f_{ref}(i,j)|_{i=1,2,\dots,7, j=1,2,\dots,40} \quad (4.20)$$

4.3 Experimental Results and Discussion

To evaluate the performance of the proposed iris recognition approach experiments have been carried out in Matlab 7.0 on Intel i3 processor (2.40 GHz) with 3 GB RAM in Windows 7 environment. The MMU2 iris dataset and IIT Delhi iris dataset have been used for experimentation. The number of persons and the number of images per person considered for experiments from the MMU2 and IIT Delhi database are tabulated in Table 4.1.

Table 4.1 Images considered for experiments from MMU2 and IIT Delhi Dataset

Dataset	Person	Images/Person	Total
MMU2	100	5	500
IIT Delhi	100	5	500

From a total number of 100 person image from each dataset, 70 images have been used as genuine and 30 images as an imposter. Among the images of genuine persons, 4 out of 5 images of each person have been used for training and 1 image for testing purpose respectively. The iris regions from individual images are segmented and unique features from the segmented iris images are extracted by using the algorithms described in section 4.2. The hybrid of neural network with city block distance described in section 4.2.6 is used for recognition of an iris image. The False Acceptance Rate (FAR) and False Rejection Rate (FRR) are computed to determine the threshold value for class separation. The ROC and CMC are used for performance assessment of the proposed iris recognition approach on both verification and identification of an iris image. In order to verify the acceptance of the proposed approach, existing iris

recognition approaches have been implemented and the results are compared with the proposed approach.

4.3.1 QPSO based Selection of Threshold Value

The linear thresholding method is used by various authors in different iris recognition algorithms in order to detect pupil region, iris region or to remove reflections, eyelashes, eyelids etc. But the efficiency of the thresholding method is dependent on the threshold value. The threshold values used by different approaches viz. Shah *et al.* (2009), Raffei *et al.* (2013) and Al-Zubi *et al.* (2007) over different datasets is given in Table 4.2. The threshold values used by different approaches viz. Shah *et al.* (2009), Raffei *et al.* (2013) and Al-Zubi *et al.* (2007) over different datasets as given in Table 4.2 are a fixed threshold value for thresholding which may not be appropriate for all kinds of iris images. The thresholding result of an input image and thresholding result by Shah *et al.* (2009), Raffei *et al.* (2013) and Al-Zubi *et al.* (2007) over MMU2 iris database are shown are in Figure 4.9.

Table 4.2 Threshold value used by Shah *et al.* (2009), Raffei *et al.* (2013) and Al-Zubi *et al.* (2007) over different datasets

Method	Threshold value	Purpose
Shah <i>et al.</i> (2009)	set threshold value '41' by $M + 25$, where M is the minimum pixel value of the image [over WVU iris dataset]	To detect pupil region
Raffei <i>et al.</i> (2013)	set threshold value '20'[over UBIRIS v2 iris dataset]	To isolate eyelashes
Al-Zubi <i>et al.</i> (2007)	set threshold value '100' and '240'[over CASIA v1 iris dataset]	To isolate eyelashes and reflections

As can be seen from the Figure 4.9 that linear thresholding used for different purpose with constant threshold value cannot appropriately identify the region of interest.

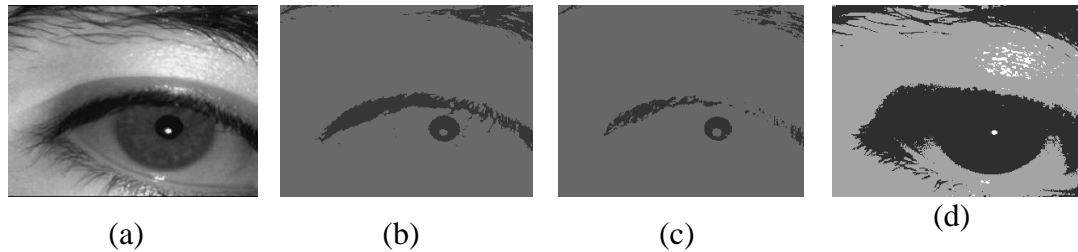


Figure 4.9 Result of thresholding (a) Original image (b) Shah *et al.* (2009) (c) Raffei *et al.* (2013) and (d) Al-Zubi *et al.* (2007) over MMU2 iris dataset

To overcome this difficulty, QPSO (as described in section 4.2) has been applied to select an optimal threshold value for linear thresholding on the input image. The results obtained by the proposed QPSO based selection of threshold value for an input image over MMU2 iris database in comparison to the threshold values used by Shah *et al.* (2009), Raffei *et al.* (2013) and Al-Zubi *et al.* (2007) is presented in Table 4.3 and in Figure 4.10.

Table 4.3 Threshold value obtained using Shah *et al.* (2009), Raffei *et al.* (2013) and Al-Zubi *et al.* (2007) approaches and the proposed QPSO based thresholding approach

Method	Threshold value	Purpose
Shah <i>et al.</i> (2009)	set threshold value '41' by $M + 25$, where M is the minimum pixel value of the image over WVU iris dataset]	To detect pupil region
Raffei <i>et al.</i> (2013)	set threshold value '20' [over UBIRIS v2 iris dataset]	To isolate eyelashes
Al-Zubi <i>et al.</i> (2007)	set threshold value '100' and '240' [over CASIA v1 iris dataset]	To isolate eyelashes and reflections
Proposed QPSO based thresholding approach	set threshold values '34', '94', '149', and '201' [over MMU2 iris dataset]	To detect eye region, isolate eyelashes, reflections and eyelids

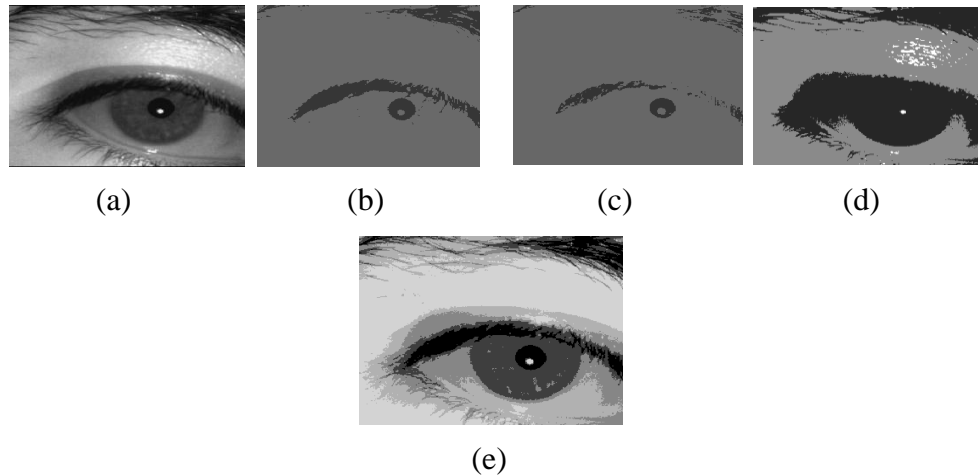


Figure 4.10 Result of thresholding (a) Original image (b) Shah *et al.* (2009) (c) Raffei *et al.* (2013) (d) Al-Zubi *et al.* (2007) and (e) Proposed QPSO based thresholding approach over MMU2 iris dataset

As can be seen from Table 4.3 that the threshold values used by different approaches *viz.* Shah *et al.* (2009), Raffei *et al.* (2013) and Al-Zubi *et al.* (2007) over different datasets are fixed threshold value. Whereas, the proposed QPSO based threshold value selection approach obtains different threshold values dynamically for different images and the thresholding result obtained by the proposed approach to detect eye region, isolate eyelashes, reflections and eyelids is superior over other approaches considered in the present work over the same datasets.

4.3.2 Segmentation Results

The proposed segmentation algorithm as described in section 4.2 has been performed on MMU2 and IIT Delhi iris datasets. The sample of iris segmentation results is shown in Figure 4.11.

The dimensions of the pupil and iris are as follows:

- i. MMU2 iris dataset
 - Average pupil radius: 20 pixels
 - Average Iris radius: 57 pixels
 - The pupil radius in the range [13 29] pixels.
 - The iris radius in the range [48 68] pixels.
- ii. IIT Delhi iris Dataset

- Average pupil radius: 33 pixels
- Average Iris radius: 82 pixels
- The pupil radius in the range [20 47] pixels.
- The iris radius in the range [64 105] pixels.

These data are summarized in Figure 4.12.

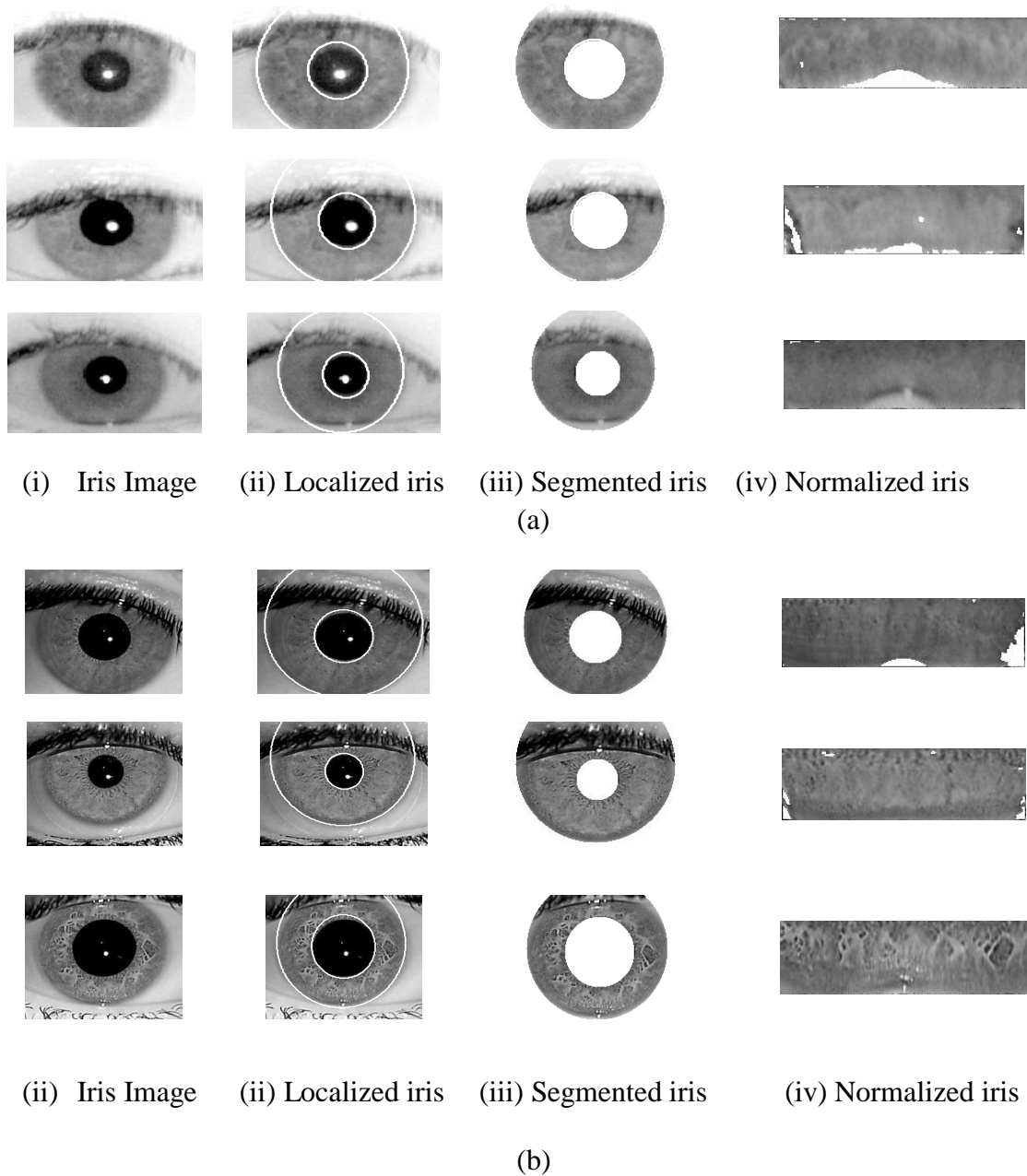
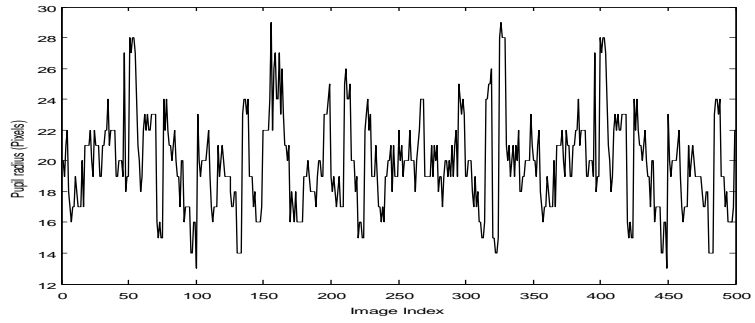
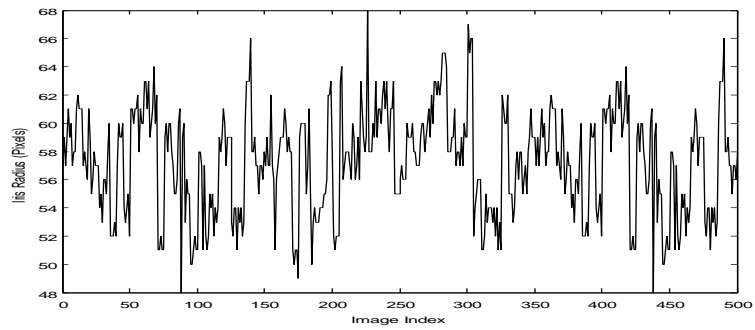


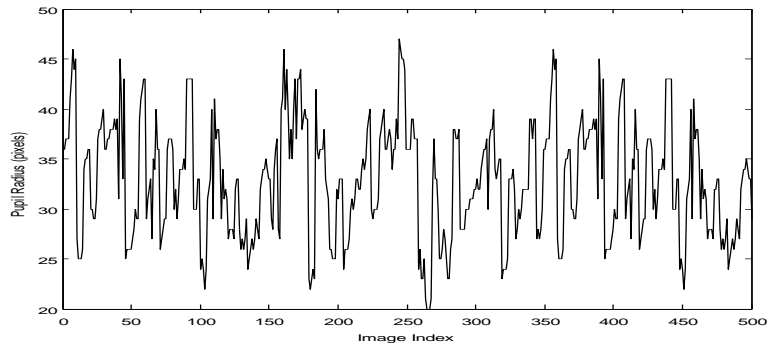
Figure 4.11 Segmentation results: (a) MMU2 Iris Dataset (b) IIT Delhi Iris Dataset



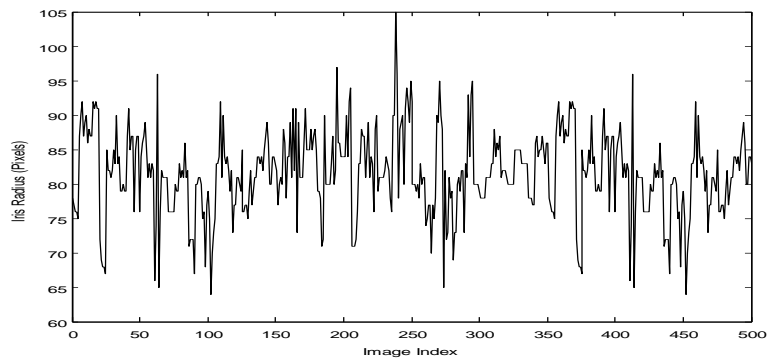
(a)



(b)



(c)



(d)

Figure 4.12 Dimensions of the pupil and iris: (a) Average Pupil radius of MMU2 dataset (b) Average iris radius of MMU2 dataset (c) Average Pupil radius of IIT Delhi Dataset (d) Average iris radius of IIT Delhi dataset

The performance of the proposed iris segmentation approach over iris recognition process is analyzed and presented in the following sections

4.3.3 Recognition Results

A hybrid feed-forward neural network algorithm with MS (city block distance) has been used for iris image recognition. The system consists of 7 feed-forward neural network for the purpose of iris recognition. The architecture and the optimal network parameters of the network are shown in Table 4.4 and Figure 4.13 respectively. The recognition result was evaluated in two modes *viz.* verification mode and identification mode.

Table 4.4 Optimal network parameters

Training function	:	'traingda'
Transfer function	:	'tansig' (hidden layer) 'Purelin' (output layer)
Epochs	:	3000
Learning rate	:	0.30
Error goal	:	0.0001
Minimum gradient	:	0.0001

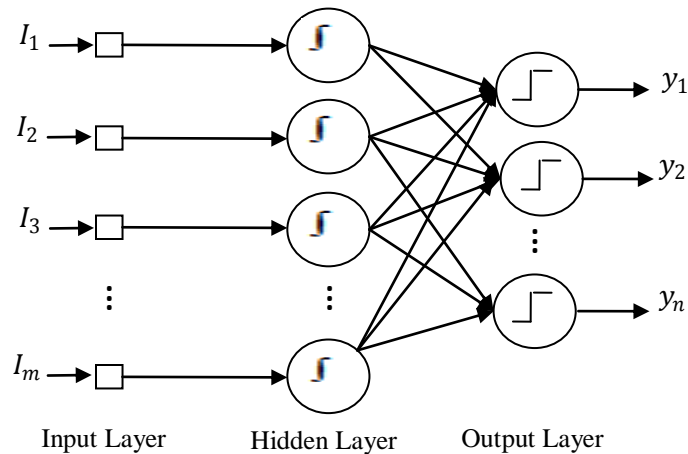


Figure 4.13 Feed-Forward network architecture: $m = 65$, $n = 10$

Verification mode: Verification mode corresponds to one-to-one matching, the system tries to match the biometric template presented by the person against a specific template already on the database. The ROC curve is used to report the verification performance of the proposed approach. It is a plot between False Acceptance Rate (FAR) versus True Acceptance rate (TAR), where, $TAR = 100 - FRR$, at different threshold. The

comparison of FAR and FRR at different threshold values over MMU2 iris dataset is shown in Figure 4.14 and can be concluded that matching score equal to 0.11 is suitable to be chosen as a threshold between intra-class and inter-class. The corresponding FAR and FRR values with 0.11 threshold value are 0.0429 and 0.0614, respectively.

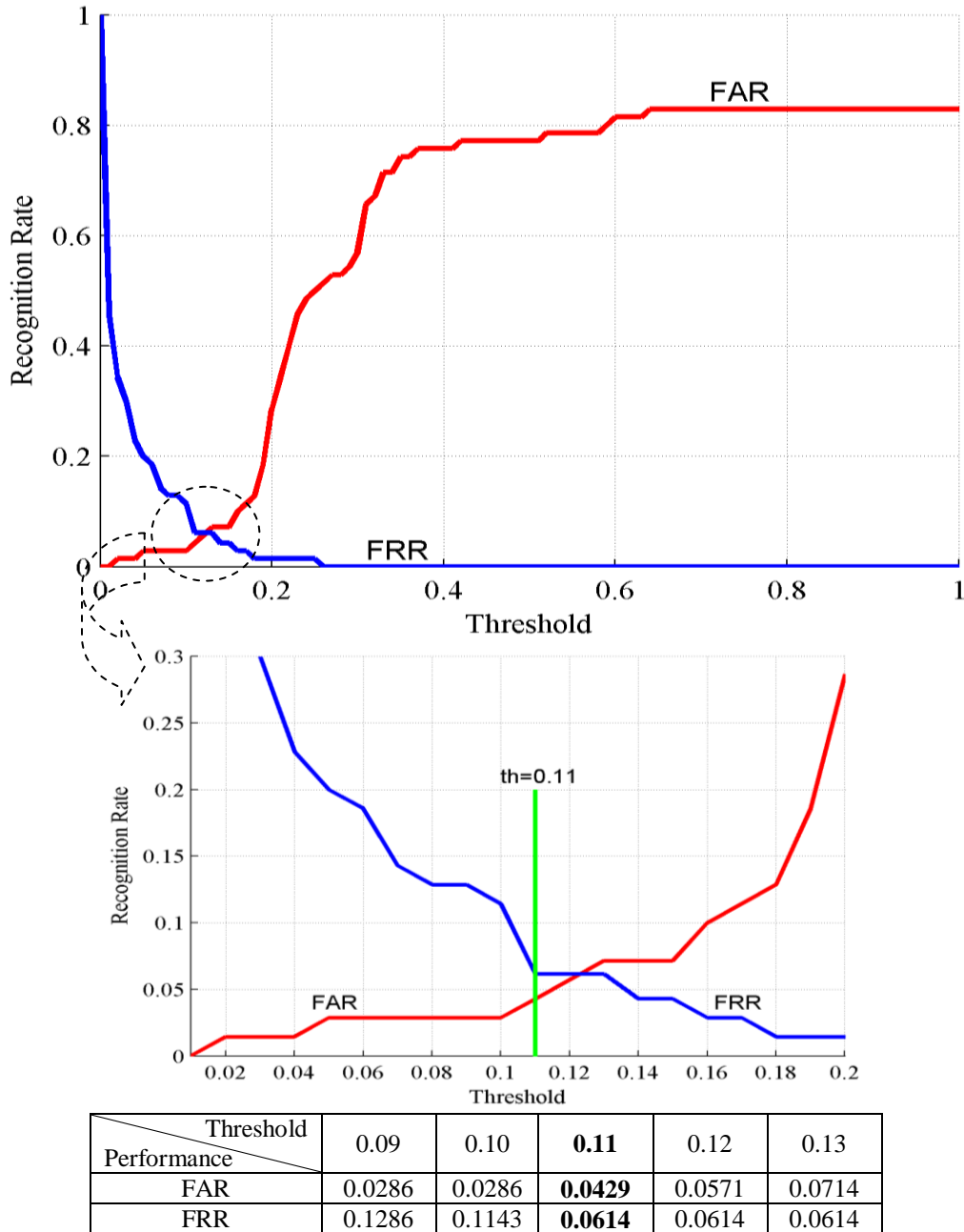


Figure 4.14 Comparison of FAR and FRR with the proposed approach over the MMU2 dataset

The influence of a number of DCT coefficients on recognition performance of the proposed approach has been tested. The experimental results with different DCT coefficients over MMU2 and IIT Delhi iris dataset are shown in Table 4.5. From the Table 4.5, it can be concluded that 65 number of DCT coefficient is suitable for verification of an individual. The proposed approach has achieved verification accuracy of 94.78% with MMU2 iris dataset and 95.51 % with IIT Delhi iris dataset. The accuracy is calculated by equation (4.21):

$$\text{Accuracy} = \left(1 - \frac{\text{FAR} + \text{FRR}}{2}\right) \times 100 \quad (4.21)$$

Table 4.5 Experimental results with different DCT coefficients over MMU2 and IIT Delhi iris dataset

No. of DCT coefficients	MMU2		IIT Delhi	
	FAR	FRR	FAR	FRR
23	0.2857	0.1207	0.0857	0.2667
65	0.0429	0.0614	0.0329	0.0571
135	0.1857	0.0345	0.1714	0.2143
233	0.2241	0.0857	0.0571	0.1714

To evaluate the proposed recognition approach on verification mode, its performances are compared with two existing iris image recognition approaches *viz.* Al-allaf *et al.* (2012) and Mozumder *et al.* (2015). These algorithms are implemented and tested on the same set of iris images. The experimental results of the comparison are presented in table 4.6. The ROC curve of the proposed recognition approach, Al-allaf *et al.* (2012) approach and Mozumder *et al.* approach on verification mode is shown in Figure 4.15. In table 4.6 the optimal FAR and FRR value (highlighted in bold) obtained by the proposed recognition approach over MMU2 dataset are 0.0429 and 0.0614, respectively. The optimal FAR and FRR value (highlighted in bold) obtained by the proposed recognition approach over IIT Delhi dataset are 0.0329 and 0.0571, respectively.

Table 4.6 Comparison results of proposed recognition approach, Al-allaf *et al.* (2012) approach and Mozumder *et al.* approach on verification mode over MMU2 and IIT Delhi dataset

Algorithm	MMU2		IIT Delhi	
	FAR	FRR	FAR	FRR
Al-allaf <i>et al.</i> (2012)	0.8571	0.0814	0.7517	0.0714
Mozumder <i>et al.</i> (2015)	0.4000	0.0286	0.3567	0.0451
Proposed recognition approach	0.0429	0.0614	0.0329	0.0571

It is observed from the Table 4.6 and ROC curve of the proposed recognition approach, Al-allaf *et al.* (2012) and Mozumder *et al.* (2015) approaches on verification mode over IIT Delhi dataset in Figure 4.15, that the proposed approach outperforms the existing approaches in terms of verification performance of the system.

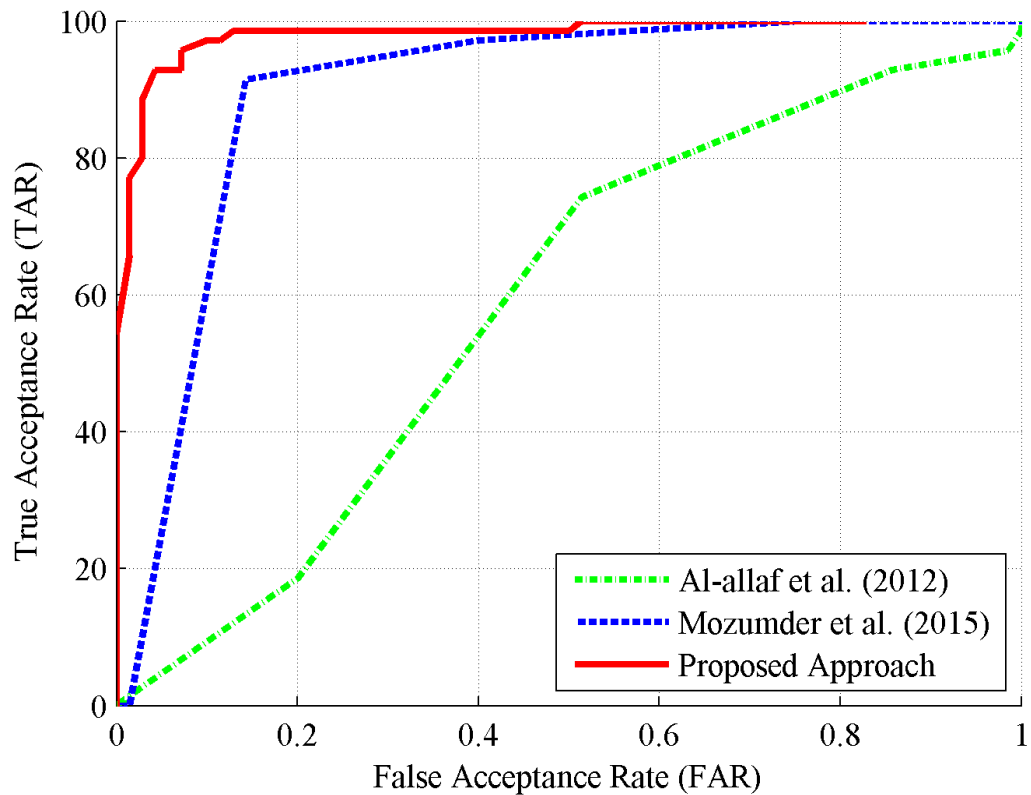


Figure 4.15 ROC curve of the proposed recognition approach, Al-allaf *et al.* (2012) and Mozumder *et al.* (2015) approaches on verification mode over IIT Delhi dataset

Identification mode: In identification mode, the proposed approach performs one-to-many comparisons. The CMC curve is used to represent the identification performance of the proposed iris recognition approach. The CMC is estimated by sorting MS between query vector and reference vectors. The genuine matching at lower rank represents the better one-to-many identification system (Raffei *et al.*, 2013). Table 4.7 represents the identification results of proposed approach over the MMU2 and IIT Delhi iris dataset. The results show that the proposed approach achieves 92.86% and 91.57% of recognition rate on MMU2 and IIT Delhi iris dataset with an average rank one respectively.

Table 4.7 Identification results of proposed approach on MMU2 and IIT Delhi Iris dataset

Rank	Recognition Rate (%)	
	MMU2 Iris Dataset	IIT Delhi Iris Dataset
1	92.86	91.57
2	95.71	95.71
3	97.14	95.71
4	98.57	96.57
5	98.57	98.57
6	98.57	99.57
7	100	100
8	100	100
9	100	100
10	100	100

The comparison results of proposed recognition approach, Al-allaf *et al.* (2012) and Mozumder *et al.* (2015) approaches on identification mode over IIT Delhi dataset are shown in Table 4.8 and Figure 4.16 as CMC curve. The results indicate that the proposed approach outperformed the existing approaches for one-to-many identification.

Table 4.8 Comparison results of the proposed recognition approach, Al-allaf *et al.* (2012) and Mozumder *et al.* (2015) approaches on identification mode over IIT Delhi dataset

Rank	Recognition rate (%)		
	Methods		
	Al-allaf <i>et al.</i> (2012)	Mozumder <i>et al.</i> (2015)	Proposed approach
1	37.42	60.00	91.57
2	41.42	60.00	95.71
3	44.28	61.28	95.71
4	45.71	64.85	96.57
5	48.57	65.71	98.57
6	48.57	76.42	99.57
7	51.28	80.00	100
8	52.85	82.85	100
9	52.87	85.71	100
10	58.57	87.42	100

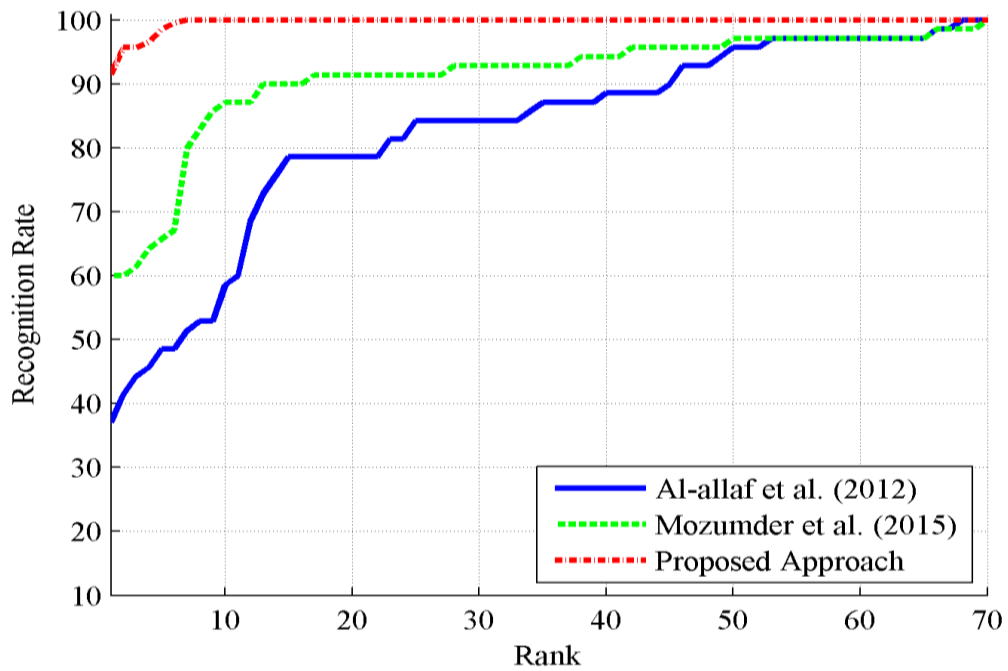


Figure 4.16 CMC curve of the proposed recognition approach, Al-allaf *et al.* (2012) and Mozumder *et al.* (2015) approaches on identification mode over IIT Delhi dataset

The CHT is tolerant to gaps in object boundary description, makes it suitable for detection of iris boundaries. But it is computationally expensive and has the time

complexity $O(n^3)$ (Sahmoud *et al.*, 2013). In the proposed hybrid segmentation approach, comprising of QPSO, Circle geometry and CHT, computational time of CHT is reduced by marginalizing the Hough space.

In the iris recognition phase the network simulation time complexity, which is a measure of number of computation, equals to $O(n.m.h^k.o.i)$, where n stands for number of training samples, m represents number of features, h^k represents the k hidden layer with h neurons in each layer, o represent number of output neurons and i is the iteration (“Neural network models (supervised)”, 2016, http://scikit-learn.org/stable/modules/neural_networks_supervised.html). If m and o are the constant, then time complexity will be $O(n.h^k.i)$. Since, neural network has single hidden layer, $k=1$. Thus, the time complexity of the proposed approach during recognition is calculated as:

$$TC = O(nh) + O(n)$$

where, $O(n)$ represents time complexity of city block distance. Therefore, total time complexity is $O(nh)$.

4.4 Chapter Summary

In this Chapter, an optimal threshold value selection method based on Quantum-behaved Particle Swarm Optimization (QPSO) for determining threshold values of a given iris image has been presented. In general different thresholding methods select the threshold values by either trial and error basis or statistical decision-making processes which are not suitable for all types of eye images. The proposed approach of threshold value selection overcomes this difficulty. A Soft Computing based hybrid ensemble of feed-forward neural network and statistical city block distance is proposed for iris recognition. The proposed approach adopts hybridization of ensemble of neural network and statistical city block distance where the task of iris recognition is compartmentalized among the networks to perform the recognition efficiently. The recognition performance both in identification and verification mode of the proposed method is analyzed and presented. The ROC and CMC curve are used to show the assessment of the approach on one-to-one and one-to-many recognition performance,

respectively. The comparative analysis of proposed approach with different existing approaches demonstrates that the proposed approach outperforms some of the existing approaches in terms of verification and identification performance of the system over the considered datasets.

In the next chapter, a Modular Neural Network match score fusion based iris image recognition approach is presented to improve the recognition performance of iris recognition system.